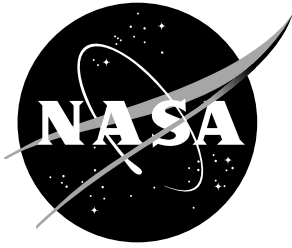


NASA/TM-2018-219812



# Automated Boundary Conditions for Wind Tunnel Simulations

*Jan-Reneé Carlson*

*Langley Research Center, Hampton, Virginia*

---

March 2018

## NASA STI Program... in Profile

Since its founding, NASA has been dedicated to the advancement of aeronautics and space science. The NASA scientific and technical information (STI) program plays a key part in helping NASA maintain this important role.

The NASA STI Program operates under the auspices of the Agency Chief Information Officer. It collects, organizes, provides for archiving, and disseminates NASA's STI. The NASA STI Program provides access to the NASA Aeronautics and Space Database and its public interface, the NASA Technical Report Server, thus providing one of the largest collection of aeronautical and space science STI in the world. Results are published in both non-NASA channels and by NASA in the NASA STI Report Series, which includes the following report types:

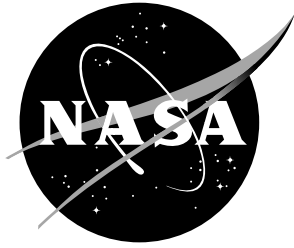
- **TECHNICAL PUBLICATION.** Reports of completed research or a major significant phase of research that present the results of NASA programs and include extensive data or theoretical analysis. Includes compilations of significant scientific and technical data and information deemed to be of continuing reference value. NASA counterpart of peer-reviewed formal professional papers, but having less stringent limitations on manuscript length and extent of graphic presentations.
- **TECHNICAL MEMORANDUM.** Scientific and technical findings that are preliminary or of specialized interest, e.g., quick release reports, working papers, and bibliographies that contain minimal annotation. Does not contain extensive analysis.
- **CONTRACTOR REPORT.** Scientific and technical findings by NASA-sponsored contractors and grantees.
- **CONFERENCE PUBLICATION.** Collected papers from scientific and technical conferences, symposia, seminars, or other meetings sponsored or co-sponsored by NASA.
- **SPECIAL PUBLICATION.** Scientific, technical, or historical information from NASA programs, projects, and missions, often concerned with subjects having substantial public interest.
- **TECHNICAL TRANSLATION.** English-language translations of foreign scientific and technical material pertinent to NASA's mission.

Specialized services also include organizing and publishing research results, distributing specialized research announcements and feeds, providing information desk and personal search support, and enabling data exchange services.

For more information about the NASA STI Program, see the following:

- Access the NASA STI program home page at <http://www.sti.nasa.gov>
- E-mail your question to [help@sti.nasa.gov](mailto:help@sti.nasa.gov)
- Phone the NASA STI Information Desk at 757-864-9658
- Write to:  
NASA STI Information Desk  
Mail Stop 148  
NASA Langley Research Center  
Hampton, VA 23681-2199

NASA/TM-2018-219812



# Automated Boundary Conditions for Wind Tunnel Simulations

*Jan-René Carlson*

*Langley Research Center, Hampton, Virginia*

National Aeronautics and  
Space Administration

Langley Research Center  
Hampton, Virginia 23681-2199

---

March 2018

The use of trademarks or names of manufacturers in this report is for accurate reporting and does not constitute an official endorsement, either expressed or implied, of such products or manufacturers by the National Aeronautics and Space Administration.

Available from:

NASA STI Program / Mail Stop 148  
NASA Langley Research Center  
Hampton, VA 23681-2199  
Fax: 757-864-6500

# Abstract

Computational fluid dynamic (CFD) simulations of models tested in wind tunnels require a high level of fidelity and accuracy particularly for the purposes of CFD validation efforts. Considerable effort is required to ensure the proper characterization of both the physical geometry of the wind tunnel and recreating the correct flow conditions inside the wind tunnel. The typical trial-and-error effort used for determining the boundary condition values for a particular tunnel configuration are time and computer resource intensive. This paper describes a method for calculating and updating the back pressure boundary condition in wind tunnel simulations by using a proportional-integral-derivative controller. The controller methodology and equations are discussed, and simulations using the controller to set a tunnel Mach number in the NASA Langley 14- by 22-Foot Subsonic Tunnel are demonstrated.

# Contents

<b>1</b>	<b>Introduction</b>	<b>4</b>
<b>2</b>	<b>Controller Package</b>	<b>5</b>
2.1	Controller Equations . . . . .	5
2.2	Tunnel and Conditions . . . . .	6
<b>3</b>	<b>Computational Method</b>	<b>9</b>
3.1	FUN3D . . . . .	9
3.2	Boundary Conditions . . . . .	9
<b>4</b>	<b>Results</b>	<b>11</b>
4.1	Empty Tunnel . . . . .	11
4.2	Model-in-tunnel . . . . .	13
<b>5</b>	<b>Summary</b>	<b>15</b>
	<b>References</b>	<b>17</b>

# Nomenclature

## *Roman letters*

A	area
a	speed of sound
$C'$	tunnel pressure calibration equation
e	control error
$k_p, k_i, k_d$	PID-controller constants
$K_{pr}$	calibration constant, 0.998
M	Mach number
$\mathcal{O}$	output of the PID-controller
p	pressure
q	dynamic pressure
Re	Reynolds number
T	temperature
t	time
U	velocity magnitude
u,v,w	Cartesian velocities
x,y,z	Cartesian directions
$p_{back}$	back pressure, $p/p_\infty$

## *Subscripts*

adjusted	accounts for position in tunnel circuit
back	back pressure
corrected	accounts for compressibility and vapor pressure
exit	at location of exit boundary
indicated	difference between upstream and downstream plenum pressures
inflow	at location of inflow boundary
min	at local of minimum area
t	total conditions
vapor	vapor pressure
$\infty$	freestream condition

## *Conventions*

CFD	computational fluid dynamics
IC	initial condition
JF	Junction Flow
PV	process variable
QCR	quadratic constitutive relation
RC	rotation correction
RH	relative humidity
SA	Spalart-Allmaras
SP	setpoint

Sta.	tunnel station
<i>Symbols</i>	
$\gamma$	ratio of specific heats, (1.4 for air)
$\mu$	bulk viscosity
$\rho$	density

# 1 Introduction

As part of the NASA Junction Flow (JF) experiment Ref. [1,2], an effort was launched to revisit the computational fluid dynamic (CFD) modeling of the flow in the NASA Langley Research Center 14- by 22-Foot Subsonic Tunnel ( $14 \times 22$ ). In the report by Rumsey et al. [3], inviscid and viscous calculations were performed on grids modeling the empty tunnel and viscous calculations using grids with the JF wing placed in the test section. For the empty tunnel simulations, the importance of high fidelity geometric descriptions was emphasized as this excerpt from Rumsey et al. [3] explains:

With JF testing taking place in the  $14 \times 22$ , considerable effort is being expended to understand CFD’s ability to model the tunnels flow characteristics. Earlier CFD work for this wind tunnel was performed by Nayani et al. [4, 5]. In Nayani et al. [4] only the high-speed leg of the tunnel was modeled. When running CFD, the as-built wind-tunnel shape (measured with laser scanning) yielded upflow angles closer to those measured in the tunnel, as compared to the as-designed shape. Wall pressures and boundary layer profiles were in reasonable agreement with experimental data. In Nayani et al. [5], the entire circuit was modeled. In the current study we do not repeat the entire circuit effort, but rather focus on simulation of the high-speed leg only. We only include the “as-built” shape, since Nayani et al. already demonstrated its importance.

Along with the importance of using the actual tunnel shape, the setting of the boundary conditions as an equally critical aspect of the computation was emphasized. Though, the work only partially examined the question of “setting the proper boundary conditions.” Rogers et al. [6] also brought this issue up and developed a calibration formula to more closely align the conditions in the CFD with the conditions in the wind tunnel. In this paper, that concept is carried one step further where the CFD is a) much more tightly coupled with the actual tunnel condition equations and b) automated.

Several factors influence the values of the boundary conditions. The inflow boundary condition is less of an issue since it is determined by the Mach number at the tunnel minimum area. Far more difficulty is involved in the determination of the outflow boundary condition. In the previous study, the flow in the “as-built” shape of the tunnel predicted separation in the diffuser at  $M = 0.2$  (unit Reynolds number of approximately 1 million/ft). The separation extended all the way downstream to the outflow boundary at which point the simulation was unable to continue due to the resulting numerical inconsistency at the outflow boundary. Modification of the grid with the addition of a constant area extension to the diffuser successfully mitigated the problem but



consequently changed what value the back pressure needed to be to retain the desired test section Mach number. Another situation that could influence and change the value of the back pressure is the addition of a model and support system in the test section. The flow in the diffuser is significantly altered by the presence of the model and would require some other value of back pressure to obtain the desired tunnel conditions.

The method proposed in this paper automates determination of the back pressure for wind tunnel simulations. The typical researcher trial-and-error technique in the solution process is removed. The method greatly reduces the time-to-solution and cost of a particular simulation. The controller and tunnel data reduction equations are described in Sec. 2. A short description of the computational method and boundary conditions are discussed in Sec. 3, and the results of using the controller on three test cases are shown in Sec. 4.

## 2 Controller Package

The method consists of several tasks: data acquisition, analyses of the data, processing by the controller and then updating the boundary conditions. The controller equations are general to most problems but the data sampling and tunnel condition equations documented herein are specific to the  $14 \times 22$  tunnel.

The controller equation and boundary condition updating is discussed in the following subsections, and the last subsection briefly describes the  $14 \times 22$  tunnel high speed leg and lists the equations used by the  $14 \times 22$  to process the data obtained from the upstream plenum chamber.

### 2.1 Controller Equations

The system uses a proportional-integral-derivative (PID) type controller,

$$\mathcal{O} = k_p e + k_i \int_0^t e(\tau) d\tau + k_d \frac{de}{dt}, \quad e = SP - PV, \quad (1)$$

where the control signal is the sum of three terms: the proportional term as a function of the control error ( $e$ ), the integral of the error, and the derivative of the error. The controller can be driven by several different variables: Mach number, dynamic pressure or Reynolds number. The setpoint (SP) is the target value of the variable driving the simulation. The process variable (PV) is the value of the variable as calculated by tunnel condition equations at each flow code iteration. The output,  $\mathcal{O}$ , using the discrete controller equation,

$$\mathcal{O}_j = k_p e_j + k_i \sum_{n=0}^j e_n + k_d (e_j - e_{j-1}), \quad e_j = SP - PV_j, \quad (2)$$

adjusts the value of the back pressure boundary condition. FUN3D samples the PV, calculates the error, integral and derivative terms at each iteration  $j$ . In this paper, the controller coefficients  $k_p$ ,  $k_i$ , and  $k_d$  are kept constant for the duration of each simulation. The boundary condition is updated using Eq. 3 at a specified (user-defined) interval.

$$p_{\text{back,new}} = (1 - \mathcal{O}_i) p_{\text{back,previous}} \quad (3)$$

The frequency of the update is dependent on the lag time of the particular simulation. The test cases in this paper used an update frequency of 1000 iterations after an initial delay of 2000 iterations. The initial delay allows for some reduction in the solution start-up transients influencing the controller. The values of the controller coefficients differ by several orders of magnitude depending on the process variable chosen. No attempt was made to *finely* tune the coefficients for this paper. Only results using the Mach number as the process variable are shown in this paper.

## 2.2 Tunnel and Conditions

A sketch of the outer shell used in the validation of the controller is the high-speed leg of the  $14 \times 22$  tunnel as shown in Fig. 1. The inflow boundary (just upstream of the screens in the tunnel) is located 70 ft upstream of the start of the test section that starts at Sta. 0. The test section is 50 ft long and is followed by a diffuser extending downstream. The diffuser is terminated at approximately Sta. 192, just prior to the first turn of the physical tunnel geometry. The ‘‘Extended diffuser’’ moves the outflow boundary 100 ft downstream via a constant area duct that starts at Sta. 192. The  $14 \times 22$  tunnel measures data from two points upstream of the test section in the plenum chamber. The first point at tunnel Sta. 711,  $[x = -59.33, y = -23.0, z = -13.4]$  ft, measures the total pressure of the tunnel flow. The second point, at tunnel Sta. 758,  $[x = -12.00, y = -10.00, z = -0.035]$  ft, measures the static pressure and temperature just upstream of the start of the test section. The location of these two data points are shown in a sketch of the tunnel plenum chamber in Fig. 2. FUN3D samples the solution every iteration from the same locations and calculates the total and static conditions required for the tunnel condition equations.

$$U|_{\text{Sta.711}} = \sqrt{u^2 + v^2 + w^2} \quad (4)$$

$$a|_{\text{Sta.711}} = \sqrt{\gamma p / \rho} \quad (5)$$

$$M|_{\text{Sta.711}} = \left[ \frac{U}{a} \right]_{\text{Sta.711}} \quad (6)$$

$$p_t|_{\text{Sta.711}} = p \left[ 1 + \frac{1}{2}(\gamma - 1) M^2|_{\text{Sta.711}} \right]^{\gamma/(\gamma-1)} \quad (7)$$

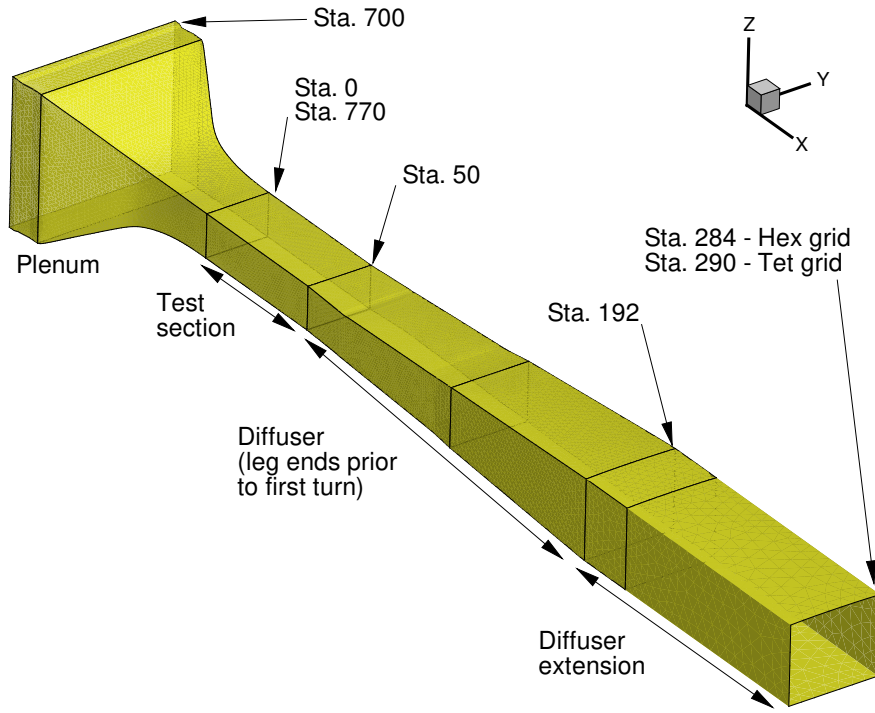


Figure 1. As-built high-speed leg of 14 × 22-foot wind tunnel.

The indicated pressure difference is adjusted per the tunnel calibration and is used to calculate a tunnel static pressure, Mach number and dynamic pressure.

$$\Delta p|_{\text{indicated}} = (p_t|_{\text{Sta.711}} - p|_{\text{Sta.758}}) \text{ [lbf/ft}^2\text{]} \quad (8)$$

$$C' = \mathcal{F}(\Delta p|_{\text{indicated}}) \quad (9)$$

$$\Delta p_\infty = C' K_{pr} \Delta p|_{\text{indicated}} \text{ [lbf/ft}^2\text{]} \quad (10)$$

$$P_{\text{adjusted}} = (p_t|_{\text{Sta.711}} - \Delta p_\infty) \text{ [lbf/ft}^2\text{]} \quad (11)$$

$$M_{\text{adjusted}} = \sqrt{5 \left( \frac{P_t|_{\text{Sta.711}}}{P_{\text{adjusted}}} \right)^{2/7} - 1} \quad (12)$$

$$q_{\text{adjusted}} = \frac{1}{2} \gamma P_{\text{adjusted}} M_{\text{adjusted}}^2 \text{ [lbf/ft}^2\text{]} \quad (13)$$

A corrected density and velocity is used to determine the tunnel Reynolds number. Each equation is annotated with the expected units of measure. In FUN3D, all the nondimensional parameters are converted into the appropriate units in order to use the same equations as the facility to the greatest extent possible.

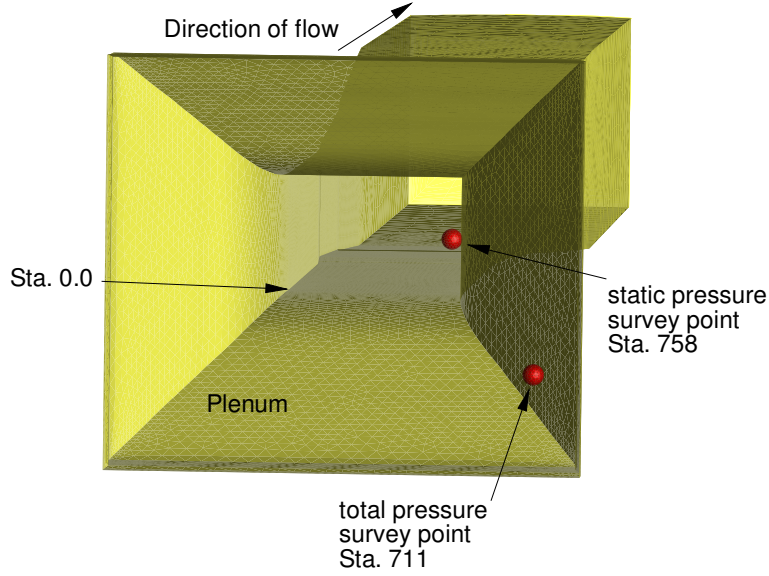


Figure 2. Schematic of the survey points in the plenum of the  $14 \times 22$  wind tunnel.

$$T|_{\text{Sta.758}} = \gamma \frac{p}{\rho} \Big|_{\text{Sta.758}} \quad (14)$$

$$T_{\text{dewpoint}} = 437.47 \frac{\log\left(\frac{\text{RH}}{100}\right) + \left(\frac{17.625T|_{\text{Sta.758}}[\text{C}]}{243.04 + T|_{\text{Sta.758}}[\text{C}]}\right)}{17.625 - \log\left(\frac{\text{RH}}{100}\right) - \left(\frac{17.625T|_{\text{Sta.758}}[\text{C}]}{243.04 + T|_{\text{Sta.758}}[\text{C}]}\right)} + 32 \text{ [F]} \quad (15)$$

$$p_{\text{vapor}} = 2.80288 + 0.0954685 T_{\text{dewpoint}} \quad (16)$$

$$+ 0.0070509 T_{\text{dewpoint}}^2 \left[ \frac{\text{lbf}}{\text{ft}^2} \right] \quad (17)$$

$$\rho_{\text{corrected}} = \left[ \frac{p_t|_{\text{Sta.711}} - 0.3789 p_{\text{vapor}}}{G T|_{\text{Sta.758}}[\text{R}]} \right] \left( \frac{p_t|_{\text{Sta.711}}}{p_{\text{adjusted}}} \right)^{-1/\gamma} \left[ \frac{\text{slug}}{\text{ft}^3} \right] \quad (18)$$

$$V_{\text{adjusted}} = \sqrt{2 \frac{Q_{\text{adjusted}}}{\rho_{\text{corrected}}} \left[ \frac{\text{ft}}{\text{s}} \right]} \quad (19)$$

$$\mu = \frac{0.0002672}{T|_{\text{Sta.758}}[\text{R}] + 198.72} \left( \frac{T|_{\text{Sta.758}}[\text{R}]}{518.69} \right)^{3/2} \left[ \frac{\text{slug}}{\text{ft}^2\text{s}} \right] \quad (20)$$

$$\text{Re} = \frac{\rho_{\text{corrected}} V_{\text{adjusted}}}{\mu} \left[ \frac{1}{\text{ft}} \right] \quad (21)$$

As used in Eqs. 14 to 21, the value of the gas constant used in the corrected density equation is  $G = 1718 \text{ [ft}^2/\text{s}^2\text{R]}$  and RH is the relative humidity. Due to the unavailability of the dew point for each data point obtained by the  $14 \times 22$  tunnel, a relative humidity is assumed and the dew point is calculated using Eq. 15 from Ref. [7].

## 3 Computational Method

### 3.1 FUN3D

FUN3D is an unstructured three-dimensional, implicit, Navier-Stokes code. Roe’s flux difference splitting [8] is used for the calculation of the inviscid terms. The method for calculation of the Jacobian was the flux function of van Leer [9]. Flux limiters were not used in any of the simulations. Other details regarding FUN3D can be found in the manual [10], as well as in the extensive bibliography that is accessible at the FUN3D Web site [11].

### 3.2 Boundary Conditions

This section discusses the determination of the inflow and outflow boundary conditions for internal flows. The typical practice for modeling the inflow in a wind tunnel simulation is to specify the total pressure and total temperature [12–14]. Setting the static pressure is most commonly used for the outflow boundary condition. Additional details on these boundary conditions (as used by FUN3D) can be found in Carlson [14]. For inviscid flow simulations, the boundary conditions can be exactly determined. The proper total conditions at the inflow and static conditions at the outflow are calculated from a set of inviscid thermodynamic relations. The Mach number at the minimum area of the tunnel, which is taken to be the freestream condition ( $M_{\min} = M_{\infty}$ ) in the simulation, determines the values of the total pressure and temperature at the inflow boundary, see Eq. 22. The following equations will use the subscript ‘min’ to designate the minimum area of the tunnel, in lieu of the subscript  $\infty$ . The discussion is applicable to internal flows in general and the use of  $\infty$  can be confusing in this context.

$$\frac{P_{t,\text{inflow}}}{P_{\min}} = \left(1 + \frac{\gamma - 1}{2} M_{\min}^2\right)^{(\gamma/\gamma-1)}, \quad \frac{T_{t,\text{inflow}}}{T_{\min}} = \left(1 + \frac{\gamma - 1}{2} M_{\min}^2\right) \quad (22)$$

The area ratio between the minimum area of the tunnel and the exit area at the end of the tunnel diffuser,  $A_{\min}/A_{\text{exit}}$ , will determine the static pressure at the outflow boundary. Newton’s method is used to solve the transcendental

equation, Eq. 23, to determine the Mach number at the exit.

$$M_{\text{exit}} \left( 1 + \frac{\gamma - 1}{2} M_{\text{exit}}^2 \right)^{\frac{1}{2} - \frac{\gamma}{\gamma - 1}} = M_{\text{min}} \left( \frac{A_{\text{min}}}{A_{\text{exit}}} \right) \left( 1 + \frac{\gamma - 1}{2} M_{\text{min}}^2 \right)^{\frac{1}{2} - \frac{\gamma}{\gamma - 1}} \quad (23)$$

The pressure ratio at the tunnel minimum location and tunnel exit location are calculated using the equations listed in Eqs. 24 and 25, respectively.

$$\frac{p_{t,\text{min}}}{p_{\text{min}}} = \left( 1 + \frac{\gamma - 1}{2} M_{\text{min}}^2 \right)^{(\gamma/\gamma - 1)} \quad (24)$$

$$\frac{p_{t,\text{exit}}}{p_{\text{exit}}} = \left( 1 + \frac{\gamma - 1}{2} M_{\text{exit}}^2 \right)^{(\gamma/\gamma - 1)} \quad (25)$$

In the absence of total pressure loss in the tunnel, i.e.,  $p_{t,\text{min}} = p_{t,\text{exit}}$ , the static pressure ratio is calculated using Eq. 26.

$$\frac{p_{\text{exit}}}{p_{\text{min}}} = \frac{(p_{t,\text{min}}/p_{\text{min}})}{(p_{t,\text{exit}}/p_{\text{exit}})} \quad (26)$$

The areas for the empty  $14 \times 22$  tunnel are listed in Table 1. When the conditions at the tunnel minimum are used as the reference and freestream conditions, then the required boundary conditions,  $p_{t,\text{inflow}}/p_{\infty}$  and  $T_{t,\text{inflow}}/T_{\infty}$  for the inflow and  $p_{\text{exit}}/p_{\infty}$  for the outflow, are completely defined for the inviscid simulation.

Table 1. Tunnel areas.

Station	Area [ft <sup>2</sup> ]
Inflow	2838.5
Minimum	316.7
Exit	850.3

Useful initial conditions for the viscous calculations are the inviscid boundary conditions determined using Eqs. 22 through 26. The degree of viscous loss is not known a priori, as discussed in the report by Rumsey et al. [3], and Rogers et al. [6], so the static pressure at the outflow boundary, i.e., back pressure or  $p_{\text{back}}$ , has to be lower than the pressure used for the inviscid simulation. In the previous study, the back pressure was manually iterated to attain the desired Mach number in the test section. Due to the tedious nature of this iteration process, only a few manual updates to the back pressure were performed before the solution was deemed “close enough.” The manual iteration process is now replaced with the PID-controller to automatically drive the back pressure to the correct level.

## 4 Results

Two grids were used for the proof-of-concept testing of the controller. The grid and initial conditions are listed in Table 2. The first configuration was an empty tunnel grid and the second configuration is the tunnel with a model and support system included. The two grids were originally constructed as mixed element grids, but were converted to pure tetrahedral elements for this study. The grids were courtesy of Henry Lee at the NASA-Ames Research Center in support of the Junction Flow project mentioned in the Introduction. The

Table 2. Parameters and initial conditions.

Configuration	Grid size (nodes)	Outflow	Inflow	
		( $p_{\text{back}}$ )	(plenum)	
		$p/p_{\infty}$	$p_t/p_{\infty}$	$T_t/T_{\infty}$
Empty tunnel	740,041	1.024	1.02828	1.008
Model-in-tunnel	4,289,293	1.01950	1.02828	1.008

empty tunnel initial conditions came from the of the inviscid tunnel boundary conditions discussed in Sec. 3.2. The empty tunnel grid was run using both the fixed and controlled back pressure. The model-in-tunnel grid was started using the final back pressure from the empty tunnel run. All solutions were computed using the FUN3D code with the Spalart-Almaras turbulence model [15] with the rotational correction [16] and QCR [17] (SA-RC-QCR2000) and were run in the steady-state mode. The reference unit Reynolds number and temperature were  $1.3148 \times 10^6$  1/ft and 590 °R, respectively. The relative humidity was set to 10%. The tunnel dynamic pressure was 57.601 lbf/ft<sup>2</sup> and the setpoint was  $M = 0.2$ .

### 4.1 Empty Tunnel

Convergence histories for several parameters using the PID-controller driven back pressure for the empty tunnel are shown in Figs. 3 and 4. The controller coefficients used are listed in Table 3.

Table 3. Controller coefficients, empty tunnel.

Process variable	$k_p$	$k_i$	$k_e$	RH
Mach number	$1 \times 10^{-1}$	$1 \times 10^{-5}$	$1 \times 10^{-6}$	10.

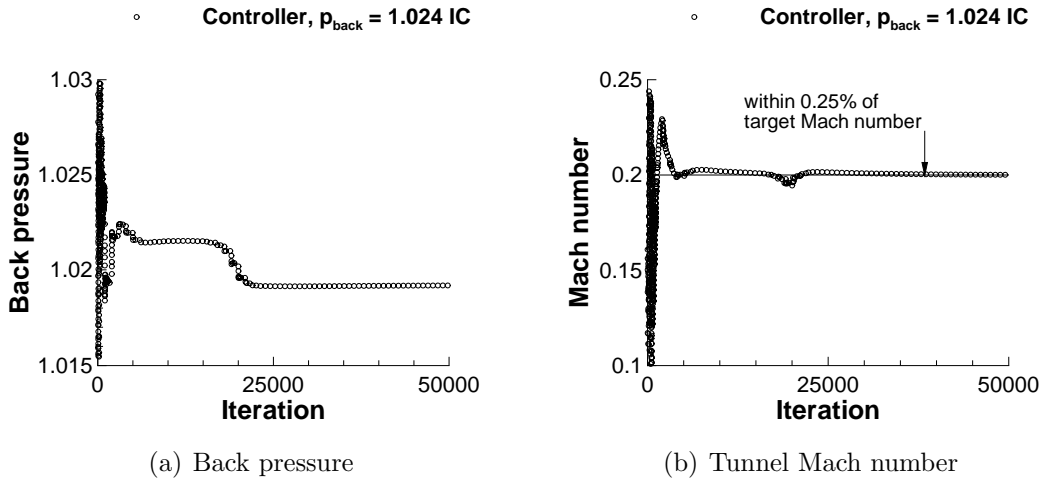


Figure 3. Simulation histories, target Mach = 0.2, empty tunnel.

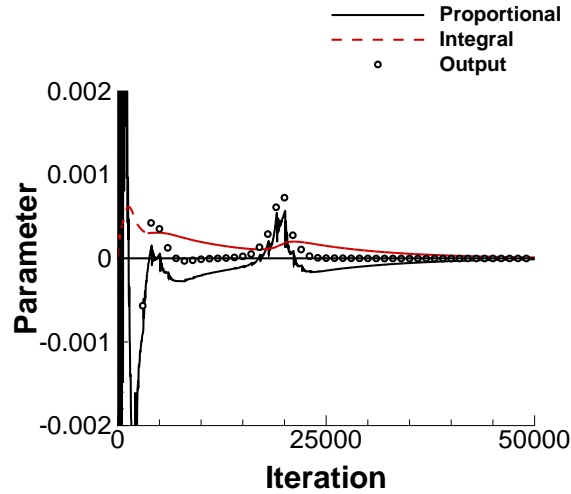


Figure 4. Controller history, target Mach = 0.2, empty tunnel.

The values calculated for the inviscid tunnel as discussed in Sec. 3.2, where used as the initial conditions. The back pressure was quickly driven to a level where the target Mach number was achieved at approximately 5000 iterations. Some time later, the separation in the diffuser changes where the controller compensates by rapidly dropping the back pressure around 20,000 iterations, see Figs. 3(a) and 3(b). The proportional term became quite active at the point as seen in the controller history plotted in Fig. 4. The error in the tunnel Mach number was reduced to 0.25% of the target Mach number by 39,000 iterations. In this situation, the controller was able to accommodate the dynamics of the developing tunnel flow and drove the back pressure to the appropriate levels.



## 4.2 Model-in-tunnel

The second configuration for testing the tunnel controller is the tunnel with a model and support system. The final boundary condition from the empty tunnel computation was used as the starting condition for the model-in-tunnel computation. The controller parameters are listed in Table 4.

Table 4. Controller coefficients, model-in-tunnel.

Process variable	$k_p$	$k_i$	$k_e$	RH
Mach number	$1 \times 10^{-1}$	$2 \times 10^{-6}$	$1 \times 10^{-6}$	10.

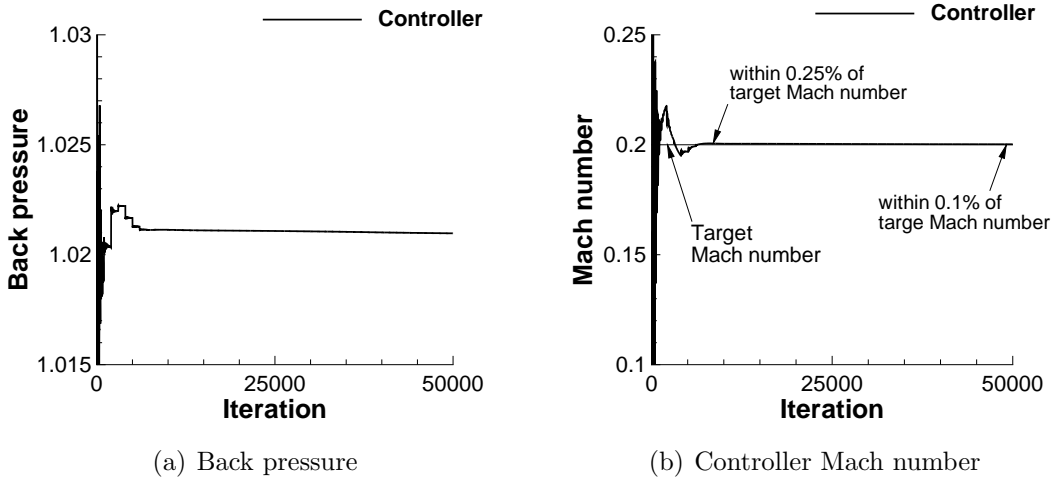


Figure 5. Simulation history, target Mach = 0.2, Model-in-tunnel.

The coefficient of the integral term was reduced by comparison with the empty tunnel configuration to slightly increase the responsiveness of the controller. The Mach number and resulting back pressure determined by the controller for empty tunnel is shown in Figs. 5(a) and 5(b). The proportional and integral terms, along with the controller output are shown in Fig. 6. By about 5000 iterations, the back pressure transient has settled down and the controller Mach number is already within a percent of the target. The margin of error was reduced to 0.25% by 8500 iterations, and 0.1% by 50,000 iterations. The proportional term drove the problem for the first 5000 iterations, as shown by the black solid line and open circle symbols matching magnitude in that interval.

Figure 7 shows Mach contours in the vertical, centerline plane cut through the tunnel for an empty tunnel and tunnel with model and support system. The model-in-tunnel configuration required a slightly higher back pressure to

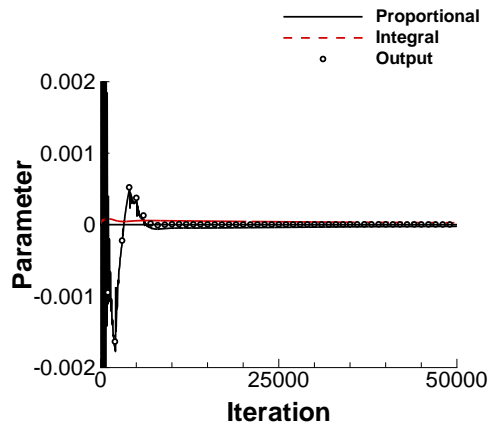
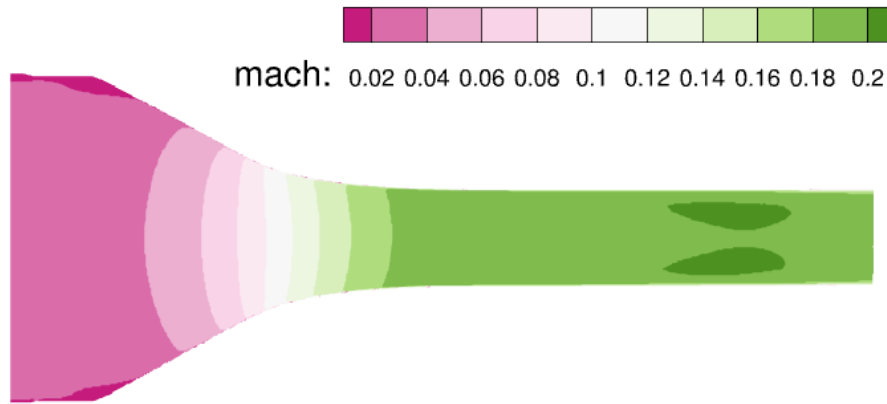
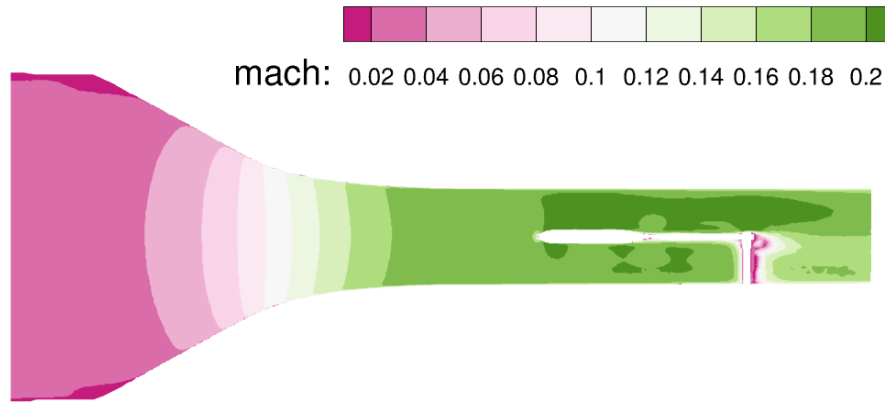


Figure 6. Controller history, target Mach = 0.2, Model-in-tunnel.



(a) Empty tunnel,  $p_{back} = 1.01950$



(b) Model-in-tunnel,  $p_{back} = 1.02116$

Figure 7. Mach number contours, vertical centerline plane, Target Mach = 0.2.

present the same adjusted Mach number as the empty tunnel. A likely reason for this shift is that the viscous losses decreased due to the lift of the model and wake of the strut changing the downstream separation and boundary layer development.

Figure 8 is the flowfield shown in Fig. 7(a) subtracted from the contours in Fig. 7(b). The back pressure for each configuration was adjusted to attain a tunnel Mach number of 0.2. In general, the difference in Mach number upstream of the model is quite small, which indicates the two tunnel simulations are operating at similar conditions.

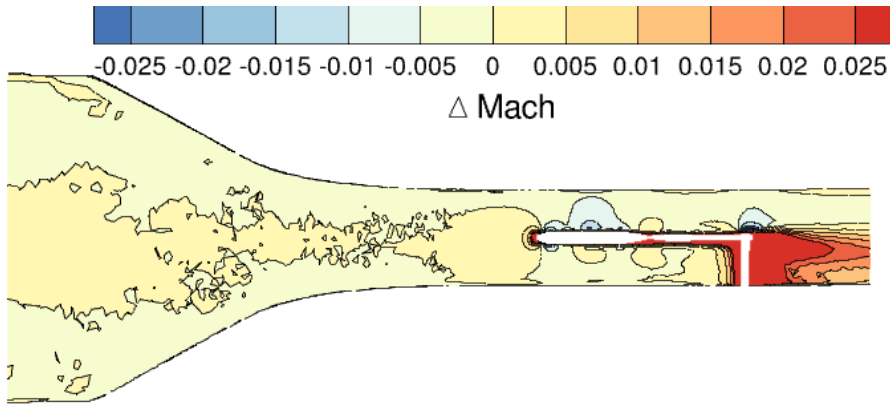


Figure 8. Difference in Mach number contours, vertical centerline plane, (empty tunnel - model-in-tunnel).

## 5 Summary

A PID-controller method to automatically determine the back pressure for a computational wind tunnel simulation was demonstrated. The controller was applied to simulations using empty and model-in-tunnel grids. The controller was able to automatically correct for flow features as they developed and successfully drive the back pressure to the requisite values to obtain the target Mach number.

## Acknowledgments

The author would like to thank Dr. Chris Rumsey, Judith Hannon, Dr. Mujeeb Malik, Henry Lee, Dr. Tom Pulliam, Dr. William Oberkampf, and other Junction Flow project participants for their invaluable discussions and feedback. In particular, the author would like to express appreciation to the author's former Branch Head, Bil Kleb, for his long standing support and encouragement. This work was supported by the NASA Transformational Tools and Technology project.



## References

1. Kegerise, M.; and Neuhart, D. H.: Wind Tunnel Test of a Risk-Reduction Wing/Fuselage Model to Examine Juncture-Flow Phenomena. NASA TM-2016-219348, NASA Langley Research Center, Nov. 2016.
2. Rumsey, C. L.; and Morrison, J. H.: Goals and Status of the NASA Juncture Flow Experiment. STO Applied Vehicle Technology (AVT) Panel, Progress and Challenges in Validation Testing for Computational Fluid Dynamics Paper Number AVT-246-03, Avila, Spain, Sept. 2016.
3. Rumsey, C. L.; Carlson, J.-R.; Hannon, J. A.; Jenkins, L. N.; Bartram, S. M.; Pulliam, T. H.; and Lee, H. C.: Boundary Condition Study for the Juncture Flow Experiment in the NASA Langley 14x22-Foot Subsonic Wind Tunnel. AIAA Paper 2017-4126, June 2017.
4. Nayani, S. N.; Sellers, W. L.; Brynildsen, S. E.; and Everhart, J. L.: Numerical Study of the High-Speed Leg of a Wind Tunnel. AIAA Paper 2015-2022, Jan. 2015.
5. Nayani, S. N.; Sellers, W. L.; Tinetti, A. F.; Brynildsen, S. E.; and Walker, E. L.: Numerical Simulation of a Complete Low-Speed Wind Tunnel Circuit. AIAA Paper 2016-2117, Jan. 2016.
6. Rogers, S. E.; Roth, K.; and Nash, S. M.: CFD Validation of High-lift Flow with Significant Wind-tunnel Effects. AIAA Paper 2000-4218, Aug. 2000.
7. <http://andrew.rsmas.miami.edu/bmcnoldy/Humidity.html>. Accessed: 2018-02-25.
8. Roe, P. L.: Approximate Riemann Solvers, Parameter Vectors, and Difference Schemes. *J. Comp. Phys.*, vol. 43, 1981, pp. 357–372.
9. van Leer, B.: Towards the Ultimate Conservative Difference Schemes V. A second order sequel to Godunov’s Method. *J. Comp. Phys.*, vol. 32, 1979, pp. 101–136.
10. Biedron, R. T.; Carlson, J.-R.; Derlaga, J. M.; Gnoffo, P. A.; Hammond, D. P.; Jones, W. T.; Kleb, W.; Lee-Rausch, E. M.; Nielsen, E. J.; and Park, M. A.: FUN3D Manual: 13.2. NASA TM-2017-219661, Aug. 2017.
11. <https://fun3d.larc.nasa.gov>. Accessed: 2017-03-20.
12. Jirasek, A.: Mass Flow Boundary Conditions for Subsonic Inflow and Outflow Boundary. *AIAA Journal*, vol. 44, no. 5, 2006, pp. 939–947.

13. Krist, S. L.; Biedron, R. T.; and Rumsey, C. L.: CFL3D User's Manual (Version 5.0). NASA TM-1998-208444, June 1998.
14. Carlson, J.: Inflow/Outflow Boundary Conditions with Application to FUN3D. NASA TM-2011-217181, Oct. 2011.
15. Spalart, P. R.; and Allmaras, S. R.: A One-Equation Turbulence Model for Aerodynamic Flows. *Recherche Aerospaciale*, vol. 1, 1994, pp. 5-21.
16. M. L. Shur, M. K. Strelets, A. K. T.; and Spalart, P. R.: Turbulence Modeling in Rotating and Curved Channels: Assessing the Spalart-Shur Correction. *AIAA Journal*, vol. 38, no. 5, 2000, pp. 784-792.
17. Spalart, P. R.: Strategies for Turbulence Modelling and Simulation. *International Journal of Heat and Fluid Flow*, vol. 21, 2000, pp. 252-263.

**REPORT DOCUMENTATION PAGE**

Form Approved  
OMB No. 0704-0188

The public reporting burden for this collection of information is estimated to average 1 hour per response, including the time for reviewing instructions, searching existing data sources, gathering and maintaining the data needed, and completing and reviewing the collection of information. Send comments regarding this burden estimate or any other aspect of this collection of information, including suggestions for reducing this burden, to Department of Defense, Washington Headquarters Services, Directorate for Information Operations and Reports (0704-0188), 1215 Jefferson Davis Highway, Suite 1204, Arlington, VA 22202-4302. Respondents should be aware that notwithstanding any other provision of law, no person shall be subject to any penalty for failing to comply with a collection of information if it does not display a currently valid OMB control number.  
**PLEASE DO NOT RETURN YOUR FORM TO THE ABOVE ADDRESS.**

<b>1. REPORT DATE (DD-MM-YYYY)</b> 01-03-2018		<b>2. REPORT TYPE</b> Technical Memorandum		<b>3. DATES COVERED (From - To)</b>	
<b>4. TITLE AND SUBTITLE</b> Automated Boundary Conditions for Wind Tunnel Simulations				<b>5a. CONTRACT NUMBER</b>	
				<b>5b. GRANT NUMBER</b>	
				<b>5c. PROGRAM ELEMENT NUMBER</b>	
<b>6. AUTHOR(S)</b> Carlson, Jan-Reneé				<b>5d. PROJECT NUMBER</b>	
				<b>5e. TASK NUMBER</b>	
				<b>5f. WORK UNIT NUMBER</b> 109492.02.07.01.01.01	
<b>7. PERFORMING ORGANIZATION NAME(S) AND ADDRESS(ES)</b> NASA Langley Research Center Hampton, Virginia 23681-2199				<b>8. PERFORMING ORGANIZATION REPORT NUMBER</b> L-20913	
<b>9. SPONSORING/MONITORING AGENCY NAME(S) AND ADDRESS(ES)</b> National Aeronautics and Space Administration Washington, DC 20546-0001				<b>10. SPONSOR/MONITOR'S ACRONYM(S)</b> NASA	
				<b>11. SPONSOR/MONITOR'S REPORT NUMBER(S)</b> NASA/TM-2018-219812	
<b>12. DISTRIBUTION/AVAILABILITY STATEMENT</b> Unclassified-Unlimited Subject Category 01 Availability: NASA STI Program (757) 864-9658					
<b>13. SUPPLEMENTARY NOTES</b> An electronic version can be found at <a href="http://ntrs.nasa.gov">http://ntrs.nasa.gov</a> .					
<b>14. ABSTRACT</b> Computational fluid dynamic (CFD) simulations of models tested in wind tunnels require a high level of fidelity and accuracy particularly for the purposes of CFD validation efforts. Considerable effort is required to ensure the proper characterization of both the physical geometry of the wind tunnel and recreating the correct flow conditions inside the wind tunnel. The typical trial-and-error effort used for determining the boundary condition values for a particular tunnel configuration are time and computer resource intensive. This paper describes a method for calculating and updating the back pressure boundary condition in wind tunnel simulations by using a proportional-integral-derivative controller. The controller methodology and equations are discussed, and simulations using the controller to set a tunnel Mach number in the NASA Langley 14- by 22-Foot Subsonic Tunnel are demonstrated.					
<b>15. SUBJECT TERMS</b> FUN3D; Aerodynamics; Computational fluid dynamics; Fluid Mechanics; Mathematics; Wind tunnel; Proportional-Integral-Derivative; Controllers; Internal flow					
<b>16. SECURITY CLASSIFICATION OF:</b>			<b>17. LIMITATION OF ABSTRACT</b>  UU	<b>18. NUMBER OF PAGES</b>  23	<b>19a. NAME OF RESPONSIBLE PERSON</b> STI Information Desk ( <a href="mailto:help@sti.nasa.gov">help@sti.nasa.gov</a> )
<b>a. REPORT</b>  U	<b>b. ABSTRACT</b>  U	<b>c. THIS PAGE</b>  U			<b>19b. TELEPHONE NUMBER (Include area code)</b> (757) 864-9658